High-Q, continuous-wave spectrometers for low temperature conductor systems

Michael J. Curtis

Franklin W. Olin College of Engineering, Needham, MA

1   Introduction

The development of NMR spectroscopic techniques was pushed significantly forward with the development of broad-band, pulsed-RF spectrometers aided by the Fast Fourier Transform (FFT). To this day, the older techniques using continuous-wave RF spectrometers are seldom used. However, continuous wave techniques may still hold a distinct advantage over pulsed techniques in regimes where the time-integral power delivered to the sample is a significant restriction, namely when performing experiments on low-temperature conductor systems. In such systems, the high-power pulses induce eddy currents which can heat the sample enough to disrupt temperature dependent measurements.

Continuous-wave techniques have the advantage of operating at much lower power, as well as the advantage that the signal which contains the results of the measurement is emitted continuously from the probe, rather than at the discrete instances where heating could occur.

Two such techniques are examined in this paper: the first using a continuous, low-amplitude RF driving signal combined with a traditional LC "tank" style probe, and the second using a tunnel diode-driven LC oscillator.

2   Background

The use of spectroscopy to study nuclear magnetic moments has been under development since the initial description of nuclear magnetic resonance in 1946 by Felix Bloch and Edward Purcell. It was noted that nuclei that had magnetic moments, resulting from non-zero intrinsic spin, were able to absorb RF energy when they were placed in a magnetic field of a specific strength. This can be explained quantum mechanically by understanding Zeeman splitting of energy levels. In an applied external field the magnetic moment of a nucleus has two eigenstates: aligned with the magnetic field (spin-up) or anti-aligned (spin-down). The difference in energy between these states is proportional to the size of the magnetic moment and the strength of the external field. A photon carrying this specific amount of energy can flip the spin of a nucleus. This specific energy corresponds to a specific frequency of photons which will induce the spin transitions. This frequency is called the Larmor frequency. The Larmor frequency is directly proportional to the strength of the external magnetic field, with the constant of proportionality called the gyromagnetic ratio, γ, which is specific to the particular nucleus.

$$\omega_{Larmor} = \gamma B_{ext} \tag{1}$$

In a system with many nuclei, one expects the relative populations of the two energy states to be proportional to $exp(-E/k_BT)$, where E is the energy of the state and T the absolute temperature. Thus there will be a population difference favoring the lower energy state, namely that with the magnetic moment aligned with the external field. This gives rise to a net magnetization of the sample aligned with the external magnetic field. Thus in principle we could study the nuclear spins by exposing the sample to radiation of a fixed frequency, ω, and slowly sweep the external

field, thus sweeping the Larmor frequency. At the point where $\omega = \omega_{Larmor}$, the RF photons will be absorbed by the sample, inducing transitions and changing the magnetization of the sample.

In a bulk system of N nuclear spins per unit voluem, where N is very large, the expectation value for the magnetization of the sample (that is, a superposition of all the N spins) evolves as a classical quantity. In general, the energy difference between the states is much smaller than the thermal energy of the system, and the Boltzman distribution of states can be expanded to a linear response. Thus the static magnetization of the sample will be linear with the applied field, as shown in Equation (2) where I is the nuclear spin quantum number[1].

$$M = \frac{N\gamma^2\hbar^2 I(I+1)}{3k_B T}B_0 = \chi_0 B_0 \tag{2}$$

We make the additional assumption that the response is *time invariant*, which simply means that if we expose the sample to the same excitation, but shifted in time by some amount Δt, then the response will shift by the same amount. With these two properties, linearity and time invariance, we can generalize the time-dependent response of the sample to Equation (3).

$$M(\omega) = \chi(\omega)B(\omega) \tag{3}$$

Where $M(\omega)$ and $B(\omega)$ are the Fourier transforms of the time-dependent magnetization and applied field, respectively. $\chi(\omega)$ is called the magnetic susceptibility of the sample, and is the Fourier transform of the impulse-response of the sample. (The impulse response is the time-dependent magnetization of the sample if it were excited by a delta function at time zero.) What this means is that if we expose the sample to a pure sinusoidal excitation in the external field, $B = B_1\cos(\omega_1 t)$, then the response of the sample would be $M = \chi(\omega_1)B_1\cos(\omega_1 t)$.

Most often, $\chi(\omega)$ is expressed in terms of its real and imaginary parts, $\chi(\omega) = \chi' - i\chi''$, where χ' and χ'' are also functions of ω. In general, these take on the forms shown in Equations () and ().

$$\chi''(\omega) = \frac{1}{2}\pi\chi_0\omega_0 f(\omega) \tag{4}$$

$$\chi'(\omega) = \frac{1}{2}\pi\chi_0\omega_0 T_2(\omega - \omega_0)f(\omega) \tag{5}$$

$f(\omega)$ is called the shape function, the form of which is shown in Equation (6). These equations are derived from assuming the restoring force and damping in the sample are linear, in other words that the spins act like a damped harmonic oscillator. T_2 is the characteristic damping timescale. In the case of the nuclear moments, it is the interaction between neighboring spins that causes this dampening, and T_2 is called the spin-spin relaxation time. ω_0 is the resonant frequency of the sample, which in the case of NMR is simply the Larmor frequency given in Equation (1).

$$f(\omega) = \frac{T_2}{\pi}\frac{1}{1+(\omega-\omega_0)^2 T_2^2} \tag{6}$$

The first NMR experiments were performed using two separate coils of wire, aligned at right angles to each other, with the external field normal to the plane defined by the axes of the coils.

One coil was used to generate a RF-field in the sample, while the other was used to measure the resultant change in the magnetization of the sample[2]. As the external field is swept, the resonant frequency of the sample changes according to Equation (1). By measuring the magnetization versus external field one is able to experimentally determine $\chi(\omega)$. A plot of amplitude of magnetization versus frequency (or external field, according to Equation (1)) is called the NMR spectrum of the sample.

NMR's ability to directly probe the magnetic susceptibility of a sample make it useful to experimentalists for studying superconductivity[3].

2.1 Pulsed Experiments

Using Fourier analysis it is possible greatly speed up the collection of the NMR spectrum. In pulsed experiments the RF signal is multiplied by a short square pulse, effectively spreading the incident radiation out in frequency space. Detectors then measure the magnetization of the sample as it relaxes back to equilibrium. The Fourier transform of this free induction decay (FID) signal reveals the NMR spectrum.

Typically, a set of balanced mixers are used to shift the frequency of the FID down to those in the audio range. This simplifies data collection and speeds up the FFT because fewer data points are needed to capture the frequency information of interest without aliasing.

Pulsed experiments differ from continuous-wave techniques in the relative power-level of the RF incident on the sample. In continuous-wave spectroscopy, care must be taken such that the incident power does not exceed a threshold in which spin transitions are induced at a rate higher than they relax back toward equilibrium, a condition known as saturation because in such a case the relative populations of spins in the sample will shift significantly, destroying the linearity of response. Because the RF-pulses are of very short time scales (~10 μs) much higher power is needed to induce enough transitions for a measurable response signal. Conducting materials exposed to this high amplitude changing magnetic field develop eddy currents which dissipate energy into the sample as heat. At high-temperature conditions this extra thermal energy is negligible due to the short time scale of the pulse. At low temperatures, however, this extra thermal energy can shift the sample's temperature significantly. Exacerbating the problem is the fact that the heating occurs at exactly the same time as measurements of the magnetization. Where heating is a large concern one may simply lower the power of the pulse. Since the sample's response is dependent on the amplitude of the pulse this places an explicit tradeoff between precise control of the sample temperature and the signal-to-noise characteristic of the experiment. While continuous-wave techniques will inevitably cause sample heating by the same mechanism as pulsed techniques, the power levels are typically orders of magnitude smaller. An additional benefit is the fact that one expects the heating to be essentially continuous, allowing the sample to reach a constant temperature in equilibrium between the induced heating and the cooling of the refrigerator.

3   Complex Impedance Measurements

One way to measure a sample's response to RF excitation is to construct a complex impedance-meter in which the impedance of a tank circuit is coupled to the susceptibility of the sample. The RF signal is then incident on the tank circuit, and the impedance can be inferred from the amplitude and phase of the reflected signal.

3.1 Theory

3.1.1 Tuning and Matching

The tank circuit is modeled as an inductance, L_0, a capacitance, C, and resistance, R, in series, and some matched reactance X_M, in parallel with them. The sample coil and capacitor are chosen such that $(L_0 C)^{-\frac{1}{2}}$ is approximately 10 MHz. We can express the impedance of the LRC branch as $Z_{LRC} = R + iX$, where X is the reactance, $\omega L_0 - 1/\omega C$. At the match condition the total impedance, $Z_T = Z_{LRC} \| iX_M = Z_0$, where Z_0 is the output impedance of the RF generator. If we assume Z_0 is purely real, we can substitute in R and X, separate real and imaginary components, and simplify to give:

$$X_M = \frac{-\left(X^2 + R^2\right)}{X} \tag{7}$$

and

$$Z_0 = \frac{R X_M{}^2}{R^2 + X^2 + X_M{}^2 + 2 X_M X} \tag{8}$$

These simplifications depend on the fact that R and X_M are positive.

Note that if L_0, C, and R are given, then X is only a function of ω, and we have a system of two variables (X and X_M). Solving the system gives

$$X^2 = Z_0 R - R^2 \tag{9}$$

Examining Equation (7), and remembering that X_M must be positive, we take X to be the negative root of Equation (9). Thus, given Z_0, L_0, R, and C, we can calculate the appropriate matched reactance, shown in Equation (10). We can also calculate the resonance frequency the match will occur at, recalling that $X = \omega L_0 - 1/\omega C$. Then, given the resonant frequency, we can calculate the inductance of the match that will equal X_M at resonance.

$$X_M = \frac{Z_0 R}{\sqrt{Z_0 R - R^2}} \tag{10}$$

Calculating an exact match is easy in principle, but building a circuit with an exact match is difficult in practice. We can model a non-ideal match by using the above formulae to calculate the appropriate match and frequency for a slightly altered Z_0. This means that the tank will be tuned to a slightly different impedance at resonance, and some power will be reflected back. To calculate the amount to change Z_0 by when calculating the match, we can measure amount of power reflected at resonance. We then multiply Z_0 by the coefficient given by Equation (11), where d is the reflected power in dB.

$$C = \frac{1 + 10^{\frac{d}{20}}}{1 - 10^{\frac{d}{20}}}$$

(11)

3.1.2 Reflection Coefficient

Far from the resonance condition, the $\chi(\omega) \approx 0$, but near resonance it is quite significant. This affects the inductance of the sample, causing a change in impedance of the tank circuit as a whole. The inductance of the sample coil is given by Equation (12).

$$L_T = L_0\left(1 + \chi' - i\chi''\right)$$

(12)

Given the susceptibility, then, we may calculate the impedance of the tank circuit for a given magnetic field in the usual way, incorporating the new inductance given above.

Given the source impedance and the impedance of the tank circuit, we can calculate the reflection coefficient for the tank circuit.

$$\rho_T = \frac{Z_T - Z_0}{Z_T + Z_0}$$

(13)

If ρ_T is therefore dependent on the susceptibility, which is in turn dependent on ω, the driving frequency and ω_0, the resonance frequency. It should be possible in principle to detect this change in reflected power as we pass through the resonance condition, however, the change in impedance of the tank circuit is often small and the reflected signal is never completely free of noise.

3.1.3 External Field Modulation

The method employed to increase sensitivity to changes in reflected power involves modulating B_0 about a center value with an amplitude much smaller than the linewidth of the resonance peak. When this field modulation is much lower in frequency than the RF signal, the reflected signal will be amplitude modulated.
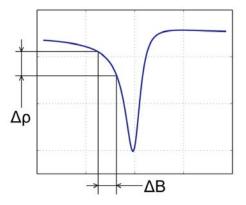

Figure 1. B-field Modulation results in modulation of the amplitude of the reflected power.

If ΔB is small, then we can assume the ρ_T versus field curve to be linear in the modulated region. This means that the magnitude of the modulation in the reflected signal, V_m, will be proportional to the derivative of the ρ_T versus field curve.

$$V_m = \frac{\partial \rho_T}{\partial B_{center}} \cdot V_{in} \Delta B \tag{14}$$

It should be noted that the signal strength in this arrangement is directly proportional to ΔB, so it is to the advantage of the experimenter to make ΔB as large as practical without entering into a regime where ρ_T can no longer be considered linear in the region defined by ΔB, as this will result in a distorted lineshape.

Additionally, the signal strength is proportional to V_{in}, the RF voltage incident on the sample. The incident RF amplitude should be determined to avoid the saturation of the spins mentioned earlier. In general this condition can be stated as

$$\gamma^2 B_1^2 T_1 T_2 < 1 \tag{15}$$

Where T_1 and T_2 are the spin-lattice and spin-spin relaxation times, respectively, and B_1 is the amplitude of the RF magnetic field in the sample coil. Typically, the B_1 versus voltage amplitude of the incident RF signal is characterized for the coil using pulsed experiments.

3.2 Experimental Setup

For purposes of this exploration, a sample of mineral oil was used. A small glass vial served as sample holder, and a coil was wound about the cylindrical vial to form the sample inductor. The inductor was wound with ~25 turns such that the impedance at 10 MHz was approximately 50 Ω. A ceramic chip capacitor of 220 pF was added in series. Matching was done experimentally by adjusting the match coil size and using a network analyzer until a sizable dip in reflected power was observed at resonance. The measured depth of the match was -37 dB. Components were soldered together and taped to a rigid surface, with a SMA connector extending from the probe.
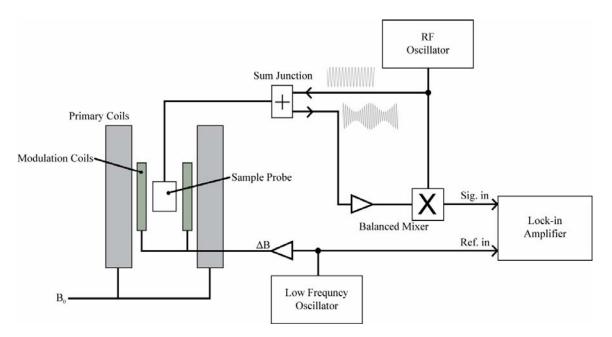
Figure 2. Impedance measurement system block diagram

The external field was generated by a large electromagnet with a Hall-probe-controlled power supply. In addition to the primary water-cooled coils, smaller modulation coils in a Helmholz configuration were used to create the field modulation mentioned in the previous section.

The driving signal is generated by an RF oscillator, which is then fed into an amplifier and split between the output to the sample and the reference signal which goes to the balanced mixer used to mix down the reflected signal. The sample output is fed through a variable attenuator to allow control over the amplitude of the RF incident on the sample as discussed previously, and connects to one input of a summing junction, which then goes to the sample coil. The other input to the summing junction actually serves as an output for the reflected signal, and connects to an RF pre-amplifier. The reflected signal received at the pre-amplifier is attenuated by -3 dB since half the reflected power goes to the other input of the summing junction and is lost. Following amplification, the reflected signal is fed into the balanced mixer, which shifts the signal down in frequency by an amount equal to the driving RF frequency. This results in any amplitude modulations in the reflected signal being demodulated such that they are now detected using a lock-in amplifier synched to the signal being delivered to the modulation coils.

The output of the lock-in amplifier is digitized and recorded as the center field is slowly swept through the resonance.
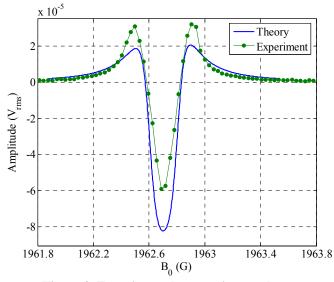
3.3   Results

Figure 3. Experimental comparison to theory

Figure 3 shows a comparison of experimental results compared with the theory derived previously. The modulation amplitude, ΔB, and spin-spin relaxation time, T_2, have been fit to the curve, and are 0.14 G and 730 μs, respectively. The plot shown above also includes a linear scaling factor which relates the proportion of the volume in the sample coil that is actually filled by sample material. Close matching between experiment and theory require that this factor be lower than expected, at 0.28, instead the 0.8 estimated by inspection of the coil.

An important consideration when making measurements is the choosing of the field modulation amplitude and the amplitude of the incident RF (to which B_1 is directly proportional).
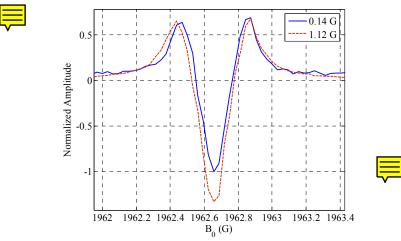

Figure 4. Comparison of lineshapes with varying field modulation amplitude (ΔB)

The effect of overmodulation is demonstrated in Figure 4. The experimental lineshape is noticeably broadened when the modulation amplitude is increased.
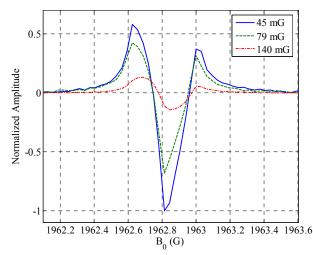
Figure 5. Comparason of lineshapes with varying B_1 amplitude

Figure 5 shows the effect of saturating the spins in the sample with an incident RF amplitude that is too high. Equation (15), using the measured parameters T_1 and T_2 for mineral oil indicates that one should limit B_1 to 4 mG, which is about an order of magnitude lower than the RF fields used in this experiment that seem to give good results. If the RF field was lowered another order of magnitude, one might expect the normalized amplitude of the lineshape to increase, however the absolute amplitude would be cut by a factor on the order of 10, increasing the number of averages required to get the same signal-to-noise ratio by a factor of 100 (since signal-to-noise goes as the square root of the number of averages). Clearly the experimenter must find the balance between cutting the amplitude so low as to harm the signal-to-noise ratio, and increasing too much as to saturate the spins.

4 Tunnel Diode Oscillator

4.1 Theory

The tunnel diode is a two terminal semiconductor device with a general current versus voltage curve that take the form shown in Figure 6.
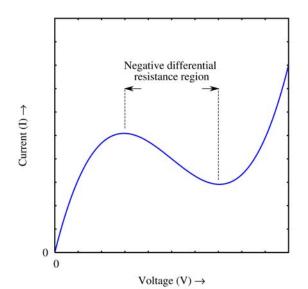
Figure 6. Typical I-V curve for a tunnel diode.

Of note is the region of negative differential resistance, this is due to the "tunnel current" of electrons and holes tunneling across the narrow depletion region which rises sharply and then drops off in the negative differential resistance region. The result is that when properly biased in this regime the tunnel diode acts like a resistor with negative resistance—an active component that can add energy to a system, instead of dissipating it like a resistor.

When placed in an LC oscillator circuit, the tunnel diode serves to negate the effects of the unavoidable resistances in components, in effect driving the LC circuit to oscillate about its own natural frequency. In a similar fashion to the impedance-meter, we can couple the oscillation frequency of the TDO to the susceptibility of the sample by placing it in the coil of the inductor. If we assume the capacitance to be constant, then the change in frequency will be proportional to the change in inductance (Equation 16.)[4]

$$\frac{\delta f}{f} \approx -\frac{1}{2}\frac{\delta L}{L} = -\frac{1}{2}\chi(\omega) \tag{16}$$

Additionally, if the tunnel diode were biased such that the center voltage was very near the peak in the tunneling current, then we expect it to behave as a marginal oscillator, and thus both frequency and amplitude would be sensitive to changes in the inductance of the sample coil. Theoretical calculation of the magnitude of this response is beyond the scope of this paper, but it was hoped that we could characterize it experimentally.

4.1.1 TDO Circuit

The TDO circuit consists of an LC tank circuit, tuned to the frequency of interest, connected to a tunnel diode which is biased to the negative differential resistance region by a bias network. It is isolated from the outside world and capacitively coupled to a pre-amplifier to measure the oscillations. A DC current source feeds the bias network and the amount of current can be used to set the bias point on the I-V curve of the tunnel diode. This arrangement is depicted in Figure 7.
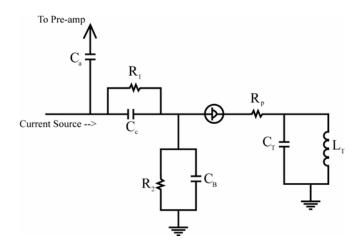
Figure 7. Tunnel Diode Oscillator Circuit

Craig Van Degrift performed an extensive study of such oscillators[5] and published approximate guidelines for the selection of the component sizes for the oscillator circuit. These guidelines are based on the desire to maximize the oscillation amplitude without dissipating too much power. If R_n is the negative resistance of the diode at the inflection point in the negative differential resistance region, ω is the LC tank circuit oscillation frequency, and Z_0 is the input impedance of the amplifier, then these guidelines are states in Equations (17) through (20).

$$R_p \approx \frac{|R_n|}{4} \tag{17}$$

$$R_2 \approx \frac{|R_n + R_p|}{4} \tag{18}$$

$$C_B \approx \frac{1000}{\omega|R_n|} \tag{19}$$

$$R_1 \sim> |R_n|$$

$$C_c \approx 10^{-5} \cdot \frac{C_B|R_n|}{Z_0} \tag{20}$$

It is important to note that Van Degrift's guidelines were designed for low temperature oscillators. Attempting to perform our analysis at room temperature, we unable to detect oscillation using values derived directly from Van Degrift's formulae. We made several modifications designed to increase the amplitude of the detected signal. We lowered the parasitic resistance, R_p, by a factor 2, increasing the amplitude of the driving. We also lowered the capacitance of the bias branch and increased the capacitance of the coupling branch, resulting in a stronger coupling between the tunnel diode and the pre-amp pickup. A comparison between the values given by the Van Degrift formulae and the actual components used in the experiment are given in Table 1.

Table 1. Comparison of Van Degrift's suggested versus our actual values

Component	Van Degrift	New Value
$|R_n|$	4.2 kΩ	4.2 kΩ
R_p	1 kΩ	500 Ω
R_2	750 Ω	300 Ω
R_1	5 kΩ	5 kΩ
C_B	5 nF	500 pF
C_c	4 pF	20 pF

4.2   Apparatus

The tunnel diode oscillation circuit was constructed on a cylindrical piece of G-10, with modulation coils wound in a Helmholz configuration to allow the external field to be modulated in a fashion similar to the detection scheme mentioned in the section on the impedance meter. Mounting the modulation coils directly on the TDO allowed the entire apparatus to be shielded in a thin layer of copper plating to help reduce noise from stray electromagnetic radiation.

4.2.1   Biasing

The bias current is provided by a simple approximation of a current source described by Van Degrift paper. In principle it is a voltage source (in our case a watch battery) which is then passed through a series of low pass filters, capacitively coupled together. The component values are exactly the same as he used, we shall simply refer the reader to Van Degrift's paper for details of the circuit. Proper biasing is accomplished by attaching leads to the terminals of the tunnel diode, measuring the voltage drop, then adjusting the current source until the desired bias point is achieved. When properly biased, oscillations from the TDO were easily detectible by using a low-noise RF preamplifier.

4.2.2   Detection

The signal from the TDO is immediately fed to a balanced mixer, and mixed with the output of a local RF oscillator operating approximately 30 kHz lower than the TDO frequency. From here, several detection schemes were attempted, depending on whether the frequency, amplitude, or both were desired to be measured.

Since the balanced mixer outputs the "sum" and "difference" frequencies of the inputs, to measure frequency of the TDO, the output of the mixer is fed through a low-pass filter, effectively cutting out the high-frequency "sum" portion of the signal. The result, the difference between the TDO and the local oscillator is fed into a frequency counter, and the TDO frequency can be deduced by simply adding the local oscillator frequency to the read-out of the frequency counter.

Measurement of the amplitude of the signal was accomplished by feeding the low-passed mixer output into a simple diode-detection circuit tuned to the frequency of interest. The output of the diode circuit was then fed into a voltmeter for measurement.
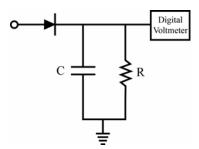
Figure 8. Diode detection circuit schematic

Measurement of both the frequency and amplitude of the signal was accomplished by splitting the output of the balanced mixer into two signals. One signal was band-passed then fed into a high-gain audio amplifier such that the amplifier saturated, effectively converting the sinusoidal oscillation into a square wave. This was then connected to the external synch on a lock-in amplifier. The other split of the mixer output was fed into the input of the lock-in amplifier, allowing the amplitude to be read off. The frequency was measured by connecting the reference channel's sinusoid output to the frequency counter, since this was synched to the square wave input.

4.2.3 Results

None of the above methods was successful in positively identifying the resonance in a sample of mineral oil in a glass vial.
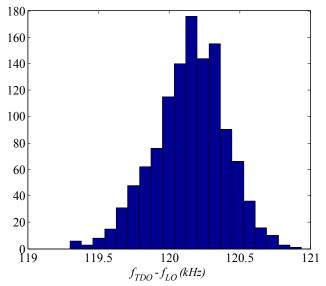

Figure 9. TDO stability; measured frequency of TDO minus local oscillator (LO) over period of 1200 seconds, measured once per second.

Figure 9 shows the stability histogram for the oscillator measured over 10 minutes. The frequency was measured at a magnetic field far from resonance, and is the output of the balanced mixer, not the absolute frequency of oscillation. The stability of the TDO signal is approximately 1 kHz in 5.6 MHz, or about one part in 10^4. $\chi(\omega)$ at resonance for mineral oil is on the order of 10^{-5}, meaning that the expected change in frequency is on the same order as the stability of the

signal. Stability, expectedly, gets worse in the condition of marginal oscillation where oscillation amplitude is also coupled to the magnetic susceptibility.

5   Discussion & Conclusions

Generally speaking, the impedance measurement benefits considerably from its simplicity. It deviates the least from the system set-up used in typical pulsed-NMR measurements and the probe used is essentially identical. The demodulation of the signal is also very straightforward. Also, the ability to build up a workable theory for the results of a complex impedance measurement from elementary principles is a major advantage of this type of measurement. The ability to directly calculate the signal-to-noise ratio of the measurement using simple equations and physical parameters of the apparatus and sample that are either easy to derive or easy to measure speeds evaluation of this type of measurement when applied to any particular problem.

In most aspects, from construction, to theory, to optimization, the tunnel diode oscillator is more complex than the impedance measurement. Although guidelines expressed as formulae do exist for selection of component values in the general circuit, it is not an exact science. Additionally, simple calculations for the signal-to-noise ratio of the measurement do not exist, since direct calculation of the oscillation properties requires numerical simulations[6] which are beyond the scope of this discussion.

Frequency stability, shown dramatically in Figure 9, is a serious problem which must be addressed before a TDO circuit can be used to make measurements of this type. The stability is on the order of 1 kHz, which is about half the width of the resonance peak in the NMR spectrum, making a precision measurement extremely difficult, even with signal averaging.

However, it should be carefully noted that this study is only a preliminary attempt to quantify the performance of these methods. Van Degrift[5] and others[4] have reported sensitivity on the order of 10^{-9} using a tunnel diode oscillator at low temperatures. Our study was performed at room temperature. Additional shielding, more rigid mounting of circuit components, and lowering the temperature should all contribute to additional signal stability. Also, the strength of the oscillations is approximately proportional to the Q-factor of the LC oscillator, which should increase significantly at low temperatures.

The Q-dependence of signal strength is also expected in the complex impedance meter, so lowering the operating temperature should benefit sensitivity in this measurement as well. The magnetic susceptibility of the sample itself is also proportional to 1/T, as shown by the well-known Curie law. However, not all properties change favorably as temperature decreases, since the spin-lattice and spin-spin relaxation times typically increase, which forces the experimenter to use a lower B_1 to avoid saturation of the spins. This is particularly important for the complex impedance measurement since the signal amplitude is directly proportional to the amplitude of the signal incident on the sample, and thus, B_1. While easily calculable for the complex impedance meter, the size of B_1 is more involved when using the tunnel diode, as the only way to affect the oscillation amplitude in the LC circuit is to make the oscillator more marginal, possibly affecting stability, or by decreasing the Q-factor of the oscillator, this cutting signal strength.

The simplicity of the complex impedance meter makes it an obvious first choice for measurements where it is sensitive enough to be used. It requires minimal changes from a pulsed-NMR setup, and very little additional detection equipment. As a first choice approach is it

also attractive because it is short work to derive the expected sensitivity from basic material properties and experimental parameters.

The tunnel diode, despite its more complicated setup, has been demonstrated to have impressive sensitivities at low temperatures, and may be able to make measurements which are beyond the reach of the complex impedance meter.

6   References

[1]   A. Abragam, *Principles of Nuclear Magnetism* (Oxford University Press, New York, 1961).
[2]   F. Bloch, W. W. Hansen, and M. Packard, Phys. Rev. **70**, 474 (1946).
[3]   I. J. Lee, S. E. Brown, W. G. Clark, et al., Phys. Rev. Lett. **88**, 017004(4) (2002).
[4]   T. J. Coffey, in *Department of Physics* (Clark University, 2003).
[5]   C. T. Van Degrift, Rev. Sci. Instrum. **46**, 599 (1975).
[6]   C. T. Van Degrift and D. P. Love, Rev. Sci. Instrum. **52**, 712 (1981).